We are IntechOpen, the world's leading publisher of Open Access books Built by scientists, for scientists

6,900
Open access books available

185,000
International authors and editors

200M
Downloads

154
Countries delivered to

Our authors are among the

TOP 1%
most cited scientists

12.2%
Contributors from top 500 universities

CLARIVATE ANALYTICS
BOOK CITATION INDEX
INDEXED

WEB OF SCIENCE™

Selection of our books indexed in the Book Citation Index
in Web of Science™ Core Collection (BKCI)

Interested in publishing with us?
Contact book.department@intechopen.com

Feasibility Study of a Passive Magnetic Bearing Using the Ring Shaped Permanent Magnets

Teruo Azukuzawa and Shigehiro Yamamoto

Additional information is available at the end of the chapter

http://dx.doi.org/10.5772/51347

1. Introduction

Magnetic bearings can suspend rotating bodies without any mechanical contact. They have advantages such as being free of dust, noise, vibration and maintenance. Some magnetic bearings are already in commercial use in specific apparatuses such as high vacuum pumps or contamination free applications [1]. However, the high cost of the control apparatus for five degrees of freedom of the rotor prevents their wide application at present. It is thus necessary to develop a low-cost magnetic bearing system.

The authors have previously reported on the characteristics of the magnetic force acting between a couple of permanent magnets [2]. A magnetic top, consisting of a couple of ring-shaped permanent magnets, can be levitated without any control while maintaining rotation by itself. This fact suggests that the magnetic top may be a potential candidate for a passive magnetic suspension system. Several efforts have been made to explain the levitation mechanism of the magnetic top. San Miguel proposed noble analytical method with complex formulas showing that a magnetic top can maintain levitation if it rotates with slight precession [3].

In this chapter, an intuitive and easy analytical method based on the equivalent coil currents model for a ring-shaped permanent magnet is proposed.

A quasi-three-dimensional analysis, in which the three-dimensional shapes and layout of the ring-shaped permanent magnets are considered to estimate the magnetic forces acting on the levitating permanent magnet, is proposed. The principle of levitation of the magnetic top and the dimensions of the permanent magnets to realise levitation are discussed using the two-dimensional equations of motion for the magnetic top.

Furthermore, simulations based on the three-dimensional equations of motion are performed to investigate the dynamic behaviour of the magnetic top. The simulated results well predict the dynamic behaviour observed in the experiments. The simulations based on

the three-dimensional analysis are used to investigate the effects of the key parameters on the levitating characteristics, such as the sizes of both the ground and rotating permanent magnets, mass of the levitating top, tilt angle of the levitating top, rotation speed and initial position related to the restoring centre.

The ability and feasibility of the magnetic top as a magnetic bearing are also discussed.

2. Analytical methods

The magnetic top is composed of a couple of ring-shaped permanent magnets magnetised in the axial direction, as shown in Figure 1. The magnetic top, equipped with a smaller ring-shaped permanent magnet (a rotor magnet), can be levitated in the magnetic field generated by the larger ring-shaped permanent magnet (a stator magnet) situated at its base, if it can maintain its rotation within a certain speed range. The levitating height is determined by the shapes and magneto-motive forces of the permanent magnets. The authors propose two types of analytical methods: (1) a quasi-three-dimensional analysis to investigate the principle of levitation and the design parameters of the permanent magnets and (2) a three-dimensional dynamic analysis to simulate the behaviour of the levitating magnetic top. The ring-shaped permanent magnet is approximated to the equivalent coil currents model in both the analytical methods.

2.1. The equivalent coil currents approximation

In the equivalent coil currents approximation, a ring-shaped permanent magnet, magnetised in the axial direction, is assumed to exist by the set of circular coil currents located at the outer and inner side surfaces of the ring-shaped permanent magnet [4]. The directions of currents in the outer and inner equivalent coils are inversed with each other, describing the axial magnetization of the permanent magnet, as shown in Figure 2. The magnitude of these equivalent side currents is determined so as to coincide with the measured magnetic field density at the pole surface of the permanent magnet in relation to the number of the assumed equivalent coils.

Figure 3 shows the analytical model based on the equivalent side currents model. The outer and inner diameters and the height of the ring-shaped permanent magnets are represented as d_{so}, d_{si} and h_s for the stator magnet and d_{ro}, d_{ri} and h_r for the rotor magnet, respectively. The angle θ is the tilt angle of the rotor magnet. The origin is set at the centre of the stator magnet. The stator magnet is located in the horizontal x–y plane and z-axis is set as the vertical direction along the axis of the stator magnet. The numbers of the equivalent side currents in both the rotor and stator magnets, indicated as one and three in Figure 3, are decided considering both the accuracy of the calculated results and the required time for computation.

2.2. Magnetic force acting on the rotor magnet

Magnetic force acting on a magnetic top can be estimated by the interaction between the magnetic field generated by the stator magnet and the equivalent coil currents of the rotor

magnet. In an analysis based on the equivalent side currents approximation, magnetic forces acting on the magnetic top can be estimated by integrating magnetic forces acting between equivalent coil currents in the rotor and stator magnets.

The magnetic force df [N] acting between two current elements dl_1 [m] and dl_2 [m] and two transporting currents I_1 [A] and I_2 [A] is estimated by the following Biot-Savart's equation:

$$df = \frac{I_1 I_2 dl_1 dl_2}{r^2} \times 10^{-7} \sin\phi \tag{1}$$

where r [m] is the distance between the two current elements and ϕ [rad] is the angle between the directions of the current elements.

Then, the magnetic force f [N] acting between two ring-shaped coil currents is estimated by integrating Equation (1) along the coil sides of the two coil currents l_1 and l_2 as follows:

$$f = \int_{l_1}\int_{l_2} df\, dl_1 dl_2 = I_1 I_2 \int_{l_1}\int_{l_2} \frac{10^{-7}}{r^2} \sin\varphi\, dl_1 dl_2 \tag{2}$$

The magnetic forces acting on the rotor magnet are estimated by integrating Equation (2) for the equivalent side currents. The x, y and z components of the magnetic forces acting on the rotor magnet F_x, F_y and F_z are estimated based on Equation (2).
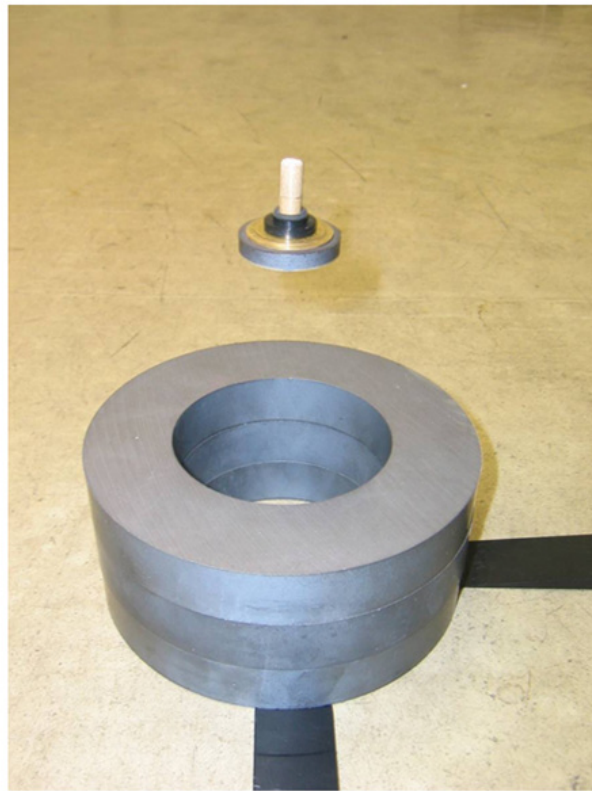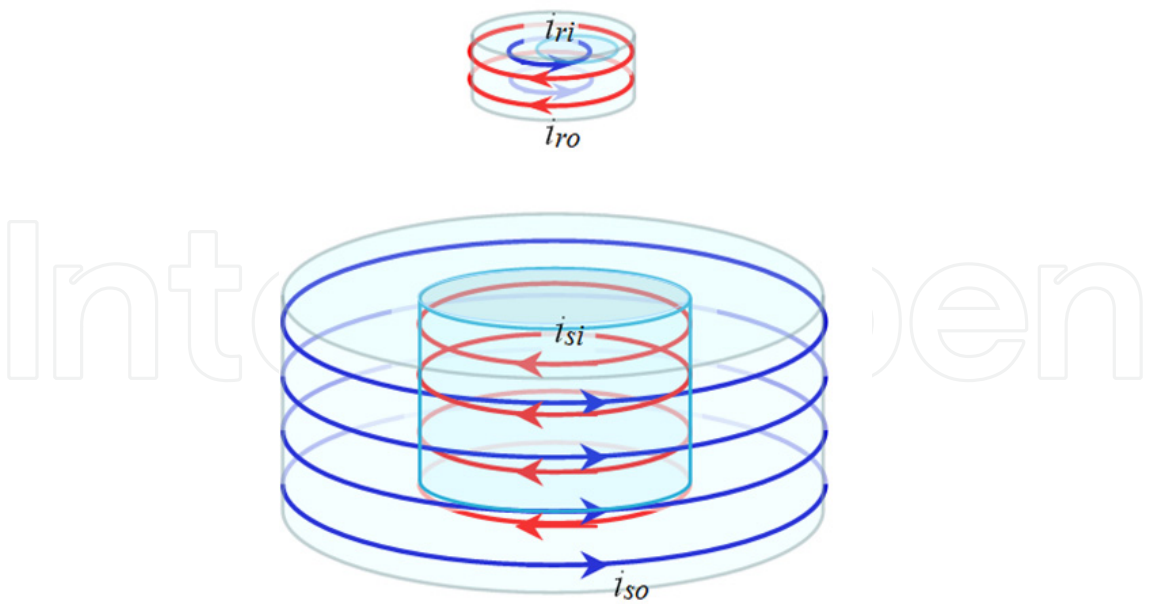

Figure 1. Experimental magnetic top.
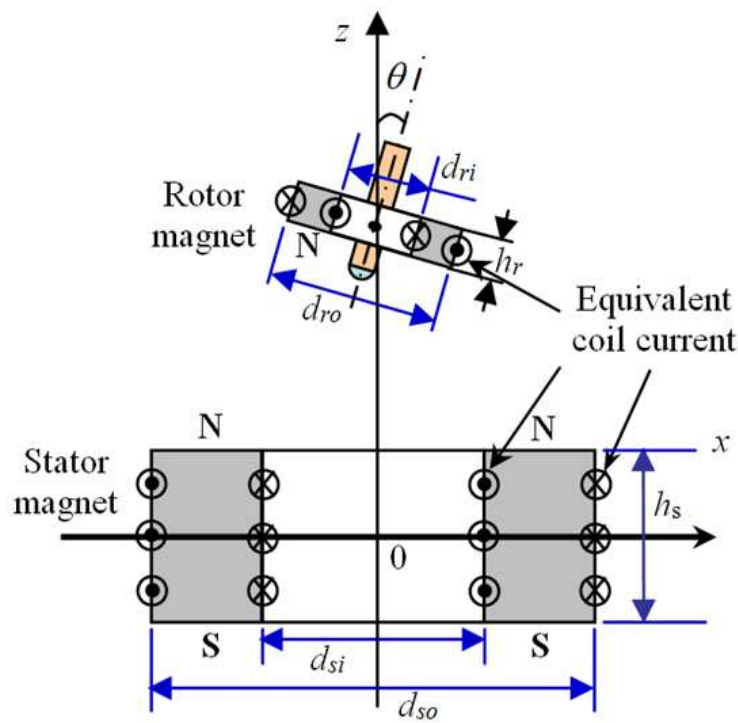
Figure 2. Equivalent side currents.

Figure 3. Analytical model.

2.3. Quasi-three dimensional analysis

Because an ideal magnetic top is considered to levitate and rotate around the z-axis, basic information can be obtained by a simple discussion on the two-dimensional motion of the magnetic top in the vertical plane including the z-axis. Hence, the authors propose the quasi-three-dimensional analysis in which the magnetic force acting on the rotor magnet is

estimated using Equations (1) and (2), considering the circular shapes and layout of the equivalent coil currents. The behaviour of the levitating magnetic top in z–x plane is estimated by the following two-dimensional equations of motion for the rotor magnet:

$$F_x = m\frac{d^2 x}{dt^2} \tag{3}$$

$$F_z = m\left(\frac{d^2 z}{dt^2} + g\right) \tag{4}$$

where F_x and F_z [N] are the magnetic forces acting on the rotor magnet in x and z directions, respectively, m [kg] is the mass of the magnetic top, g [m/s^2] is the acceleration due to gravity and (x, z) are the coordinates of the centre of the rotor magnet. Here, Equation (4) indicates that the vertical acceleration is derived from the difference between the vertical component of the magnetic force due to the stator magnet and the gravity force acting on the rotor magnet.

The quasi-three-dimensional analysis is used to investigate the principle of levitation of the magnetic top and determine with a short computing time the parameters of the magnetic top such as the sizes of the stator and rotor magnets and the levitation height.

2.4. Three-dimensional dynamic analysis

Because the quasi-three-dimensional analysis provides the design parameters of a magnetic top, behaviour of the magnetic top is investigated by a simulation based on three-dimensional dynamic analysis considering rotation of the magnetic top. Behaviour of the magnetic top can also be estimated by the equations of motion on the angular moment of the rotor magnet, considering three-dimensional layout of the stator and rotor magnets, the tilt angle of the rotor magnet and the mechanical inertia of the rotor magnet.

When the magnetic top is rotating, the angular momentum force I_{Top} will act around the axis of the rotating magnetic top. The momentum force I_{Top} can be expressed as Equation (5), where m is the mass of the levitating magnetic top, r_{ro} and r_{ri} are the outer and inner radius of the ring-shaped rotor magnet. Angular momentum vector around the axis of the rotating magnetic top L_n at a time t_n can be expressed as Equation (6), where ω is the angular velocity of the magnetic top. The incremental angular momentum $d\vec{L}$ in an infinitesimal time dt is expressed as Equation (7), where $\vec{N}$ is the moment caused by magnetic force acting on the rotor magnet. The angular momentum vector $\vec{L}_{n+1}$ at time $t_{n+1} = t_n + dt$ is expressed as Equation (8):

$$I_{Top} = m\left(r_{ro}^{2} + r_{ri}^{2}\right)\Big/2 \tag{5}$$

$$L_n = I_{Top} \times \omega \tag{6}$$

$$d\vec{L} = dt \times \vec{N} \tag{7}$$

$$\vec{L}_{n+1} = \vec{L}_n + d\vec{L} \tag{8}$$
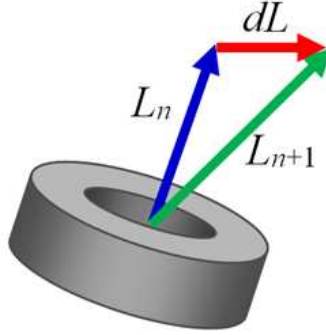
Figure 4. Angular momentum of a top

The moment $\vec{N}$ in Equation (7) corresponds to torque and can be estimated by the magnetic force acting on the rotor magnet with a calculation based on the equivalent coil currents model. The motion of the magnetic top can be simulated using the following equations by the 4th order Runge-Kutta method:

$$t_{n+1} = t_n + h \tag{9}$$

$$k_1 = h\,f(t_n,\,v_n) \tag{10}$$

$$k_2 = h\,f(t_n + h/2,\,v_n + k_1/2) \tag{11}$$

$$k_3 = h\,f(t_n + h/2,\,v_n + k_2/2) \tag{12}$$

$$k_4 = h\,f(t_n + h,\,v_n + k_3) \tag{13}$$

$$v_{n+1} = v_n + (k_1 + 2\,k_2 + 2\,k_3 + k_4)/6 \tag{14}$$

where h is the incremental time. In this analysis, the aerodynamic damping effects are neglected for easy calculation.

3. Levitating characteristics of a magnetic top based on quasi-three-dimensional analysis

3.1. Principle of levitation of a magnetic top

To investigate levitation characteristics intuitively, the authors have proposed a so-called 'magnetic force map' that shows the magnetic force acting on the rotor magnet at each mesh point in the magnetic field generated by the stator magnet. Magnetic forces at the mesh points above the stator magnet are shown in the vector diagram. Because the vertical component of the magnetic force is deducted by the weight of the levitating top, we can observe the net force acting on the top at a glance.

Table 1 shows the parameters of the analytical model used in this chapter. These parameters are for the experimental model introduced in Figure 1. The magnitude of current in each equivalent side current is determined to be equal to the magnetic field density at the surface of the permanent magnets and the measured values for the ferrite permanent magnets used in the experiments. Considering the thickness of the permanent magnets, the number of the equivalent current coils is set to be 2 for the rotor magnet and 24 for the stator magnet in the simulation. Each circular coil current is simulated as a set of 72 linear current elements. These parameters are determined considering the accuracy of calculated results and the required time for computation.

	Rotor magnet	Stator magnet
Outer diameter d_o [mm]	30	134
Inner diameter d_i [mm]	12	75
Thickness h [mm]	5	60
Magnitude of equivalent current I_{eq} [A/mm]	286	286
Mass m [g]	20.37	-
Tilt angle θ [deg]	-	1
No. of equivalent coils	2	24
No. of current elements in an equivalent coil	72	72

**Table 1.** Parameters used in simulation

Figure 5 shows the magnetic force map calculated for the parameters given in Table 1. The figure shows the distribution of the magnetic force acting on the rotor magnet at each mesh point in the vertical plane including the z–x plane. Although the magnetic force map displays the force distribution in a two-dimensional plane, the magnetic forces are calculated considering three-dimensional shapes and layout of the equivalent side currents.

Figure 5(a) shows the magnetic force map in case the tilt angle of the rotor magnet is zero, that is, the rotor magnet is laid out horizontally in the area above the stator magnet. This figure shows that the force distribution is not uniform in the space above the stator magnet. There are two singular points along the z-axis: points A (0, 99.5) and B (0, 91.5) (Figure 5(a)). At point A, the magnetic forces acting on the rotor magnet are stable in the vertical direction but unstable in the horizontal direction. On the contrary, at point B, the magnetic forces acting on the rotor magnet are unstable in the vertical direction but stable in the horizontal direction. These results show that the magnetic top cannot levitate when its axis is parallel to the vertical axis; this result accords with the Earnshaw's theorem.

Figure 5(b) shows the magnetic force map when the tilt angle of the rotor magnet θ is set to 1° in $x < 0$ to −1° in $x > 0$. This figure shows that there is a point where the magnetic forces acting on the rotor magnet are stable in the both horizontal and vertical directions, as shown by the point C (0, 99.5) in Figure 5(b). In other words, the magnetic forces will guide the rotor magnet to the equilibrium point C, named as the 'restoring centre' in this chapter.

The quasi-three-dimensional analysis shows that there is no restoring centre when the tilt angle of the rotor magnet is 0, but a slight tilt angle such as 1° brings the restoring centre into existence. These results suggest that a magnetic top equipped with a ring-shaped permanent magnet can levitate in the space above a stator ring-shaped permanent magnet if it rotates with a slight precession.


(a) $\theta = 0°$, rotor magnet is horizontal.   (b) $\theta = 1°$ with respect to z-axis.
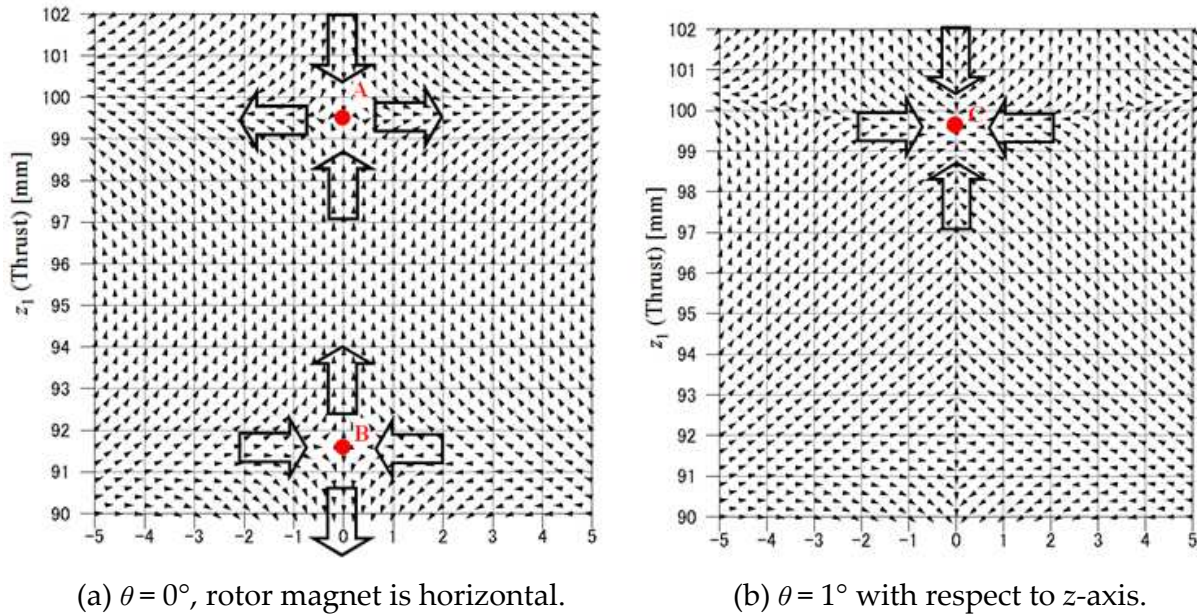
Figure 5. Magnetic force map for different tilt angles θ of a levitating magnetic top.

3.2. Simulation to investigate the behaviour a magnetic top

To confirm the validity and effectiveness of quasi-three-dimensional analysis using the magnetic force map, dynamic behaviour of the rotor magnet is investigated by computer simulation based on the equations of motion introduced in the previous section. To make intuitive discussions, a dynamic simulation using two-dimensional equations of motion, Equations (3) and (4), is performed. In this simulation, the tilt angle of the rotor magnet is set to $\theta = 1°$ in the area $x < 0$ and to $-1°$ in the area $x > 0$.
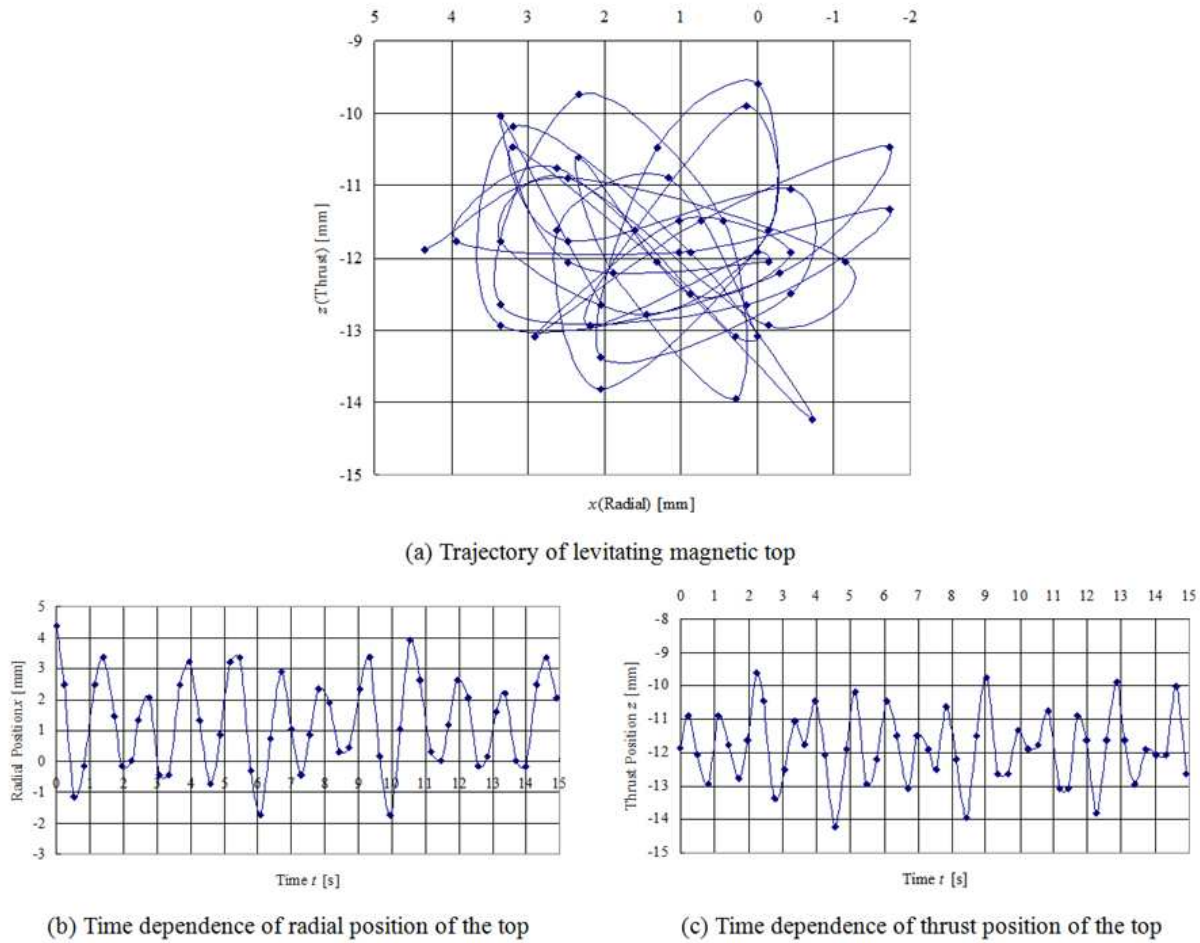
Figure 6 shows the simulated behaviour of the centre of the rotor magnet for 10 s starting from the point (1, 98.5), which is 1 mm apart in both x and z directions from the restoring centre (0. 99.5). The simulated time trajectory of the centre of the rotor magnet (Figure 6(a)) shows that the rotor magnet levitates in the area of ±1 mm in both vertical and horizontal directions from the restoring centre. The bottom left point of this rectangular space is the initial position of the rotor magnet. These results tell us that the magnetic top is swaying around the restoring centre and the range of swaying motion is determined by the initial position of the magnetic top with regard to the restoring centre. Figures 6 (b) and (c) show the time dependencies of radial and vertical motions of the centre of the rotor magnet. From these figures, we find that the frequencies of radial and vertical motions are 1.45 Hz and 1.13 Hz, respectively.

(a) Trajectory of the centre of the rotor magnet.

(b) Time dependency of radial motion.

(c) Time dependency of vertical motion
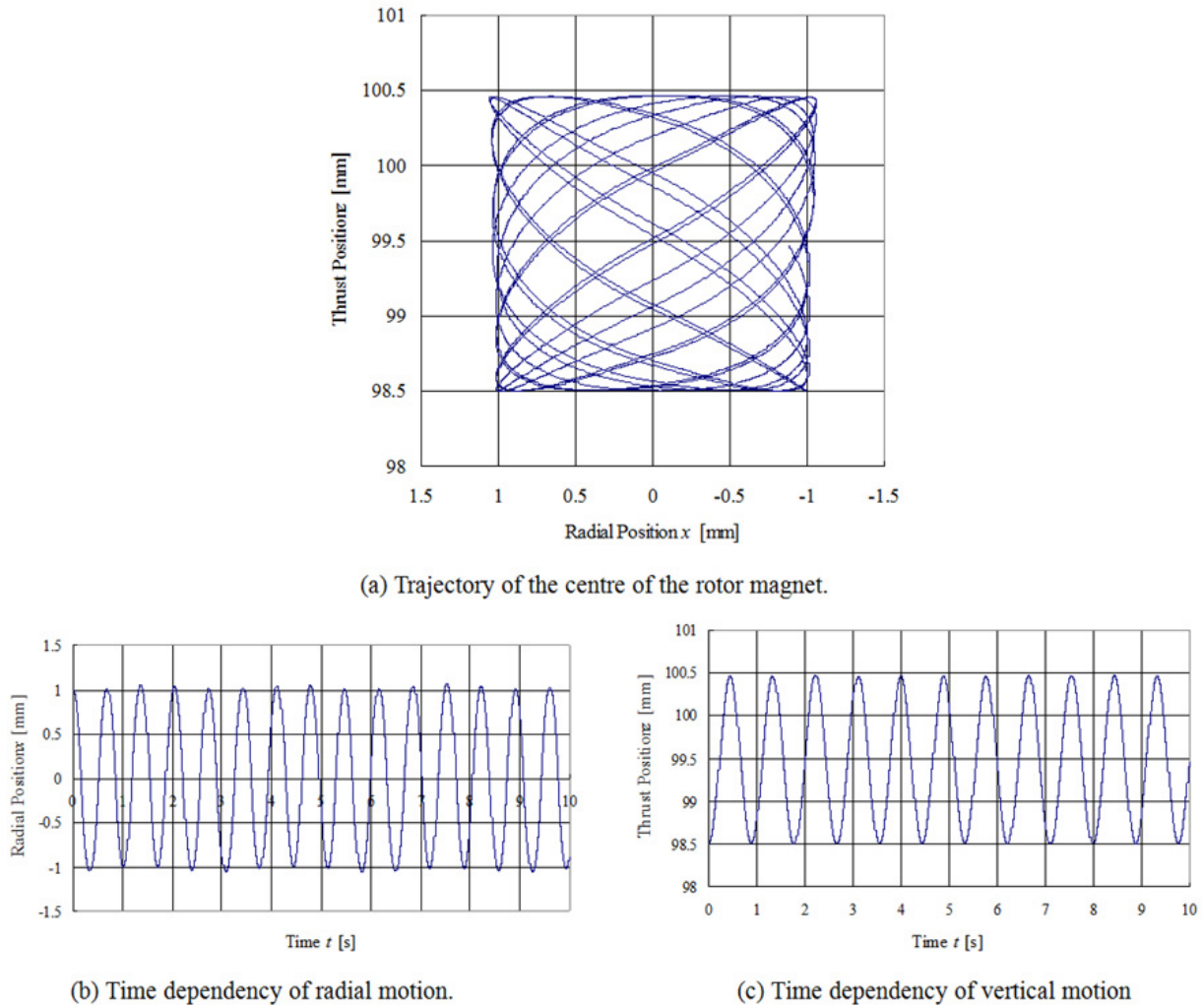
Figure 6. Simulated behaviour of the centre of the rotor magnet based on two-dimensional analysis.

3.3. Validity of the quasi-three-dimensional analysis

To verify the validity of the above analytical results, experiments are performed using the test model. The dimensions of the rotor and stator magnets used in the test model are listed in Table 1. The weight of the top is adjusted to 20.37 g using a dummy weight. Behaviour of the levitating magnetic top is recorded using a video camera from the y direction. The levitation height of the centre of the rotor magnet is about 100 mm above the centre of the stator magnet. The digital image information is obtained using motion capture software 'Pv Studio 2D demo' and the software 'Graph Scan 1.8' are used to obtain Figure 7. The frame size and frame interval of the obtained video data are 640 × 480 pixels and 30 flames per second. However, finally obtained frame interval using the above software is 4 frames per second.

(a) Trajectory of levitating magnetic top

(b) Time dependence of radial position of the top

(c) Time dependence of thrust position of the top

Figure 7. Measured behaviour of the magnetic top in the test model.

Experiment is performed according to the following steps : (1) place a non-magnetic plate on the pole surface of a stator magnet, (2) rotate a magnetic top on the plate at the centre of a stator magnet, (3) lift the plate with rotating top slowly until a magnetic top is pulled into the restoring centre. There are some hurdles to clear these steps. A magnetic top should be rotate at the exact centre of the stator magnet in a certain rotating speed range to clear step (2). Lift force should be less than vertical magnetic force acting on a top from the stator magnet to clear step (3). A magnetic top is rotated by fingers and the plate is lifted by hand in our experiment. Then, it is difficult to obtain experimental data of the same conditions.

Figure 7 shows the measured trajectory of the centre of the rotor magnet for 15 s. In Figure 7, the origin of x and z coordinates is the centre of the picture captured by the camera. In Figure 7(a), dots indicate the positions of the rotor magnet centre measured every 0.25 s, *i.e.* 4 frames per second, and a smoothing line connects these dots in sequential order. The smoothing line in Figure 7(a) does not show the swaying motion correctly; however, we can observe that the rotor magnet levitates and sways in the range of ±3 mm in radial direction and ±2.3 mm in vertical direction. In the experiment, it is difficult to start rotation of the magnetic top at the designated initial point. Figure 7(a) suggests that the initial positions of

the rotor magnet in this experiment were 3 mm and 2.3 mm apart from the restoring centres in x and z directions, respectively. Figures 7 (b) and (c) demonstrate the time dependence of the radial and vertical motions in 15 s. These figures show that the frequencies of swaying motion are about 0.75 Hz in radial direction and about 1.05 Hz in vertical direction. These test results are compared to the calculated ones in Table 2.

	Measured	Calculated
Levitation height [mm]	100	99.5
Frequency of radial swaying [Hz]	0.75	1.45
Frequency of vertical swaying [Hz]	1.05	1.13

Table 2. Comparison between analysis and experimental data

In spite of low accuracy of the measured data and difficulties in reenacting experiments in the same condition, the analysed levitation height and the frequency of vertical swaying are well in accordance with the experimental values. However, the analysed frequency of radial swaying is about twice the experimental value. This difference seem to be derived from assumptions in the two-dimensional analysis such as the constant tilt angle of the rotor magnet. Simulated results for various tilt angles showed that the magnitude of the tilt angle significantly affects the radial motion, but does not affect the vertical motion of the rotor magnet. Furthermore, the analysis is based on two-dimensional equations of motion, and three-dimensional behaviour of the magnetic top in the experiment is measured as two-dimensional video information.

These results show that the fundamental parameters of a magnetic top, such as levitation height and dimensions of the permanent magnets, can be determined well using the quasi-three-dimensional analysis.

3.4. Levitating area and parameters of the magnets

Figure 8 shows the magnetic force map for the test model shown in Table 1. The tilting angle of the rotor magnet is set as ±1°. This figure shows that a tilting magnetic top, located within the red dotted lines and named as the 'levitating area', will be guided by the magnetic force along the direction of vectors towards the restoring centre A (0, 0, 99.5). Although the levitating area is shown as a two-dimensional area in this figure, the real shape of the levitating area is conic.

The size and shape of the levitating area are closely related to the dimensions of the permanent magnets and the tilting angle of the rotor magnet. Figure 9 shows the relationship between the shape and size of the levitating area and the parameters of the permanent magnets. The effects of precession are considered to set the tilt angle θ to −1° in $x > 0$ and to 1° in $x < 0$. The conical shape of the levitating area is approximated by the rectangular area bounded by the green coloured dotted line in Figure 8 [5].
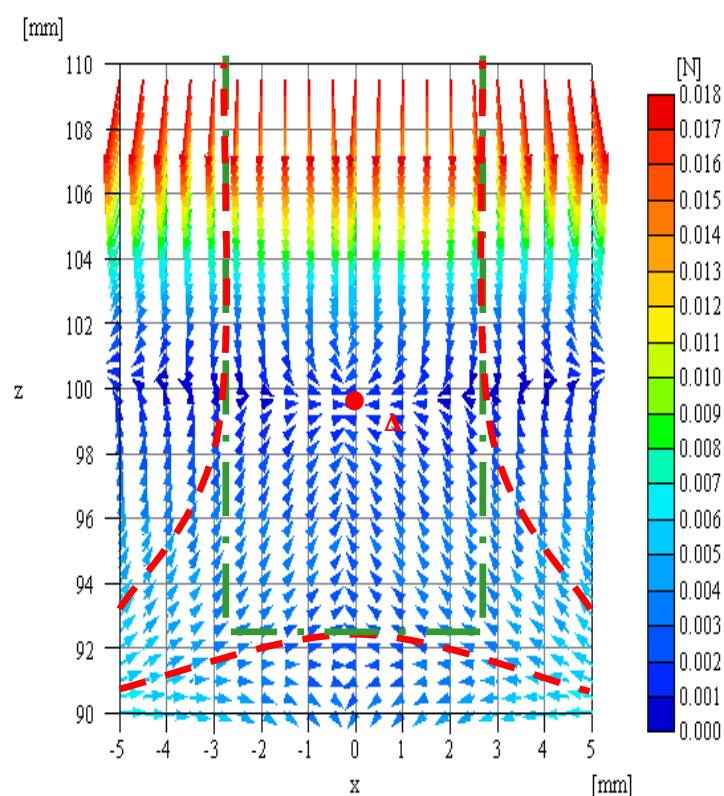
**Figure 8.** Levitating area of a magnetic top tilted by 1°.

Figure 9(a) shows the levitating areas and the restoring points for the various inner diameters of the rotor magnet d_{ri}. When the inner diameter of the rotor magnet increases, the restoring point becomes higher and the levitating area becomes narrower in the radial direction and wider in the thrust direction. These results indicate that relatively well radial bearing characteristics can be obtained by a rotor magnet with a large inner diameter. On the contrary, relatively well thrust bearing characteristics can be obtained by a rotor magnet with a smaller inner diameter.
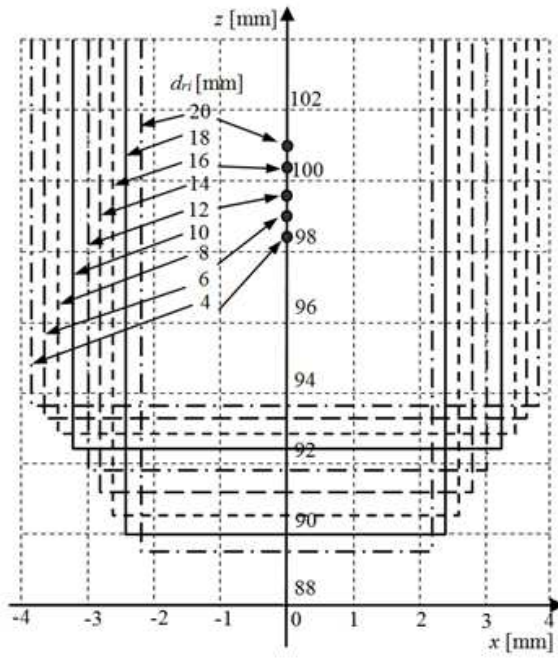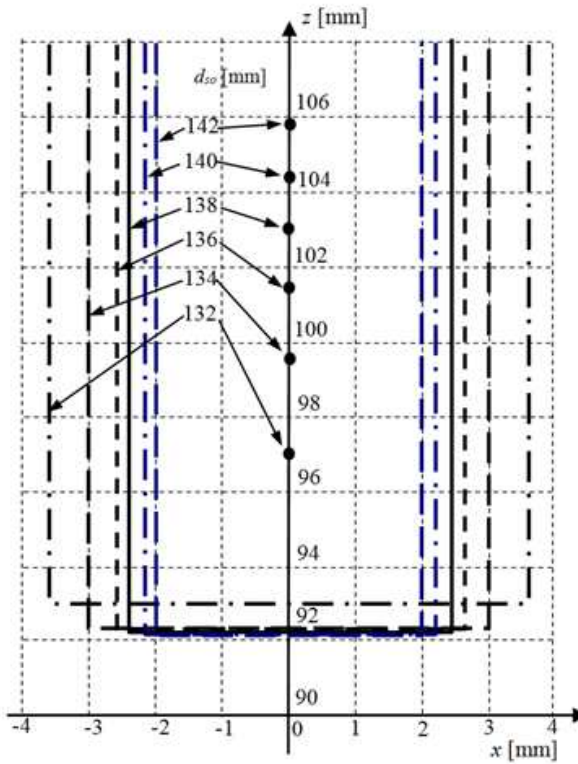
(a) Levitating areas vs. inner diameter of the rotor magnet.
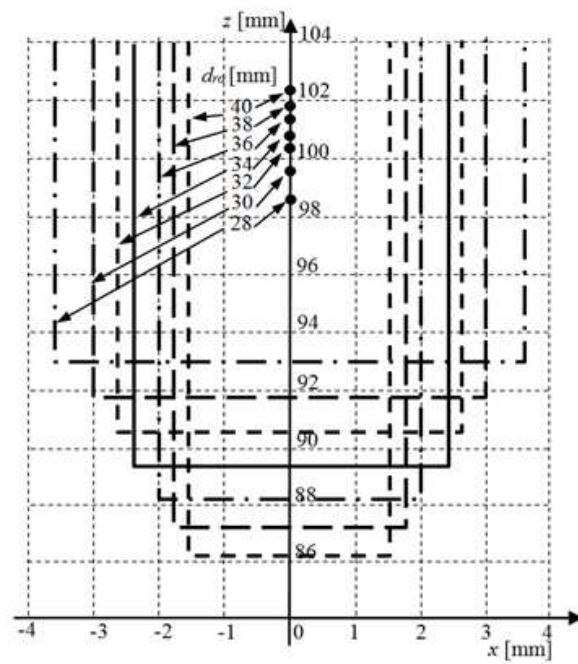
(b) Levitating areas vs. outer diameter of the rotor magnet.
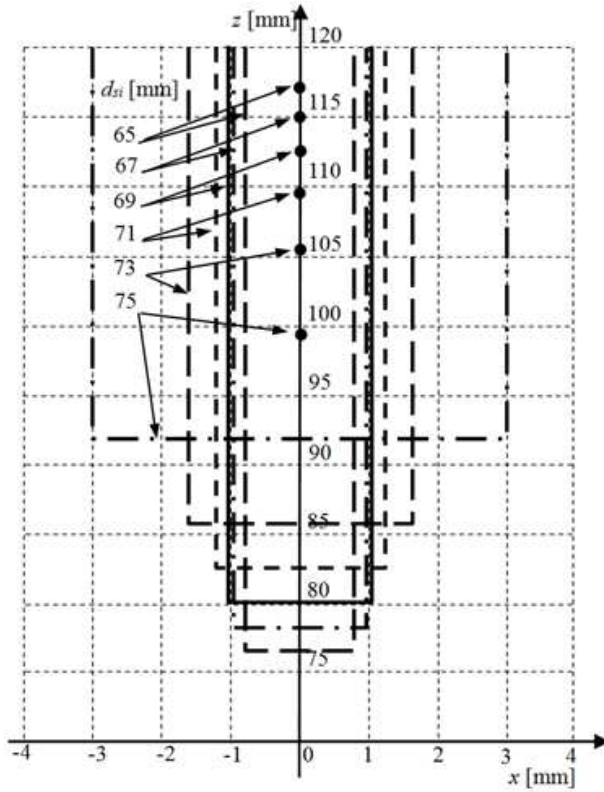
(c) Levitating areas vs. inner diameter of the stator magnet.

(d) Levitating areas vs. outer diameter of the stator magnet.

Figure 9. Relationship between the shape and size of the levitating area and the parameters of the permanent magnets.

Figure 9(b) shows the levitating areas and the restoring points in the case where the outer diameter of the rotor magnet d_{ro} changes. When the outer diameter of the rotor magnet

increases, the restoring point becomes higher and the levitating area becomes narrower in the radial direction and wider in the thrust direction. These results state that relatively well radial bearing characteristics can be obtained by a rotor magnet with a large outer diameter. On the contrary, relatively well thrust bearing characteristics can be obtained by a rotor magnet with a smaller outer diameter.

Figure 9(c) shows the levitating areas and the restoring points in case where the inner diameter of the stator magnet d_{si} changes. When the inner diameter of the stator magnet increases, the restoring point becomes lower and the levitating area becomes wider in the radial direction and narrower in the thrust direction. These results show that relatively well radial bearing characteristics can be obtained by a stator magnet with a smaller outer diameter. On the contrary, relatively well thrust bearing characteristics can be obtained by a stator magnet with a larger outer diameter.

Figure 9(d) shows the levitating areas and the restoring points in the case where the outer diameter of the stator magnet d_{so} changes. When the outer diameter of the stator magnet increases, the restoring point becomes higher and the levitating area becomes narrower in the radial direction. The outer diameter of the stator magnet hardly affects the axial height of the levitating area. These results indicate that relatively well radial bearing characteristics can be obtained by a stator magnet with a large outer diameter. The thrust bearing characteristics are not changed by the outer diameter of the stator magnet.
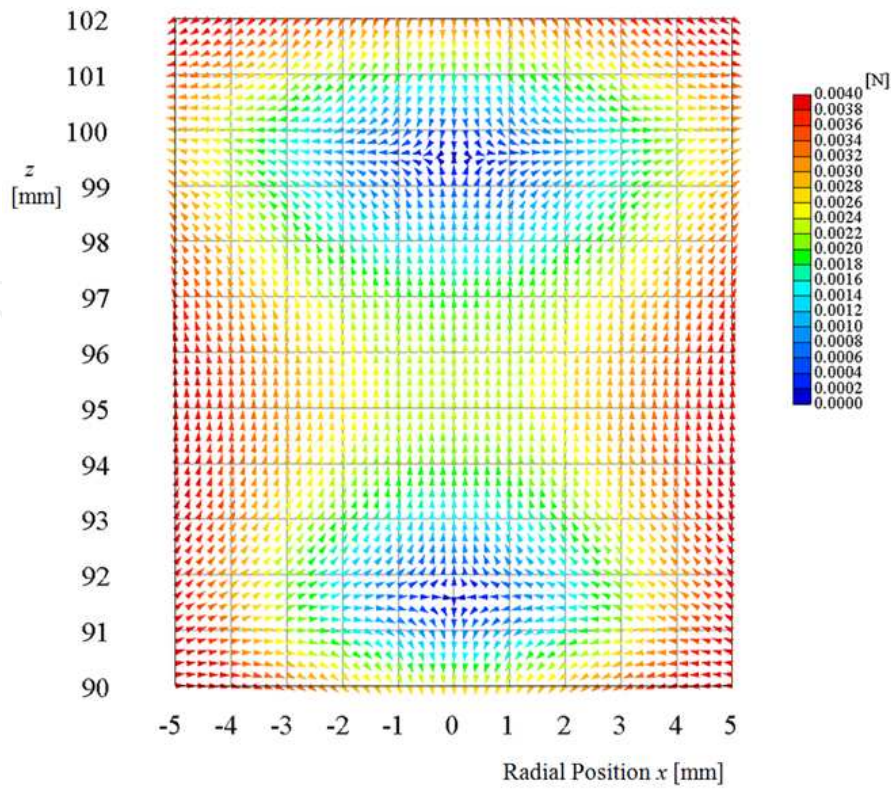
3.5. Levitating area and tilt angle of the magnets

As mentioned in the previous section, the tilting of a rotor magnet is essential in a magnetic top. In this section, relations between the shapes of the levitating area and the tilt angle of the rotor magnet are discussed.

Figure 10 shows the magnetic force map with levitating areas for different tilt angles of the rotor magnet. Figure 10(a) shows the magnetic force map when the tilt angle of the rotor magnet is zero. The magnetic forces acting on the rotor magnet are stable in the vertical direction but unstable in the radial direction at the upper singular point (0, 99.5). On the contrary, the magnetic forces acting on the rotor magnet are unstable in the vertical direction but stable in the radial direction at the lower singular point (0, 91.5). In this case, there is no levitating area because there is no restoring centre.

Figure 10(b) shows the magnetic force map when the tilt angle of the rotor magnet is $\theta = 0.4°$, i.e. $\theta = 0.4$ in the area $x < 0$ and $\theta = −0.4$ in the area $x > 0$. Figures 10(c) and (d) show the magnetic force maps when the tilt angle of the rotor magnet is $\theta = 0.8°$ and $\theta = 1.2°$, respectively. Figures 10 and 8, showing the case of $\theta = 1.0°$, illustrate the fact that the levitating area becomes wider when the tilt angle becomes larger up to 1.2°, while the magnitude of restoring force around the restoring centre becomes saturated. We can intuitively observe considering the behaviour of a normal top that a magnetic top with a very large tilting angle will not levitate. Figure 10 also shows that the height of the restoring centre does not change by the tilt angle of the rotor magnet.

(a) The magnetic force map when the tilt angle is zero.

(b) The levitating area when the tilt angle is 0.4°.

(c) The levitating area when the tilt angle is 0.8°.
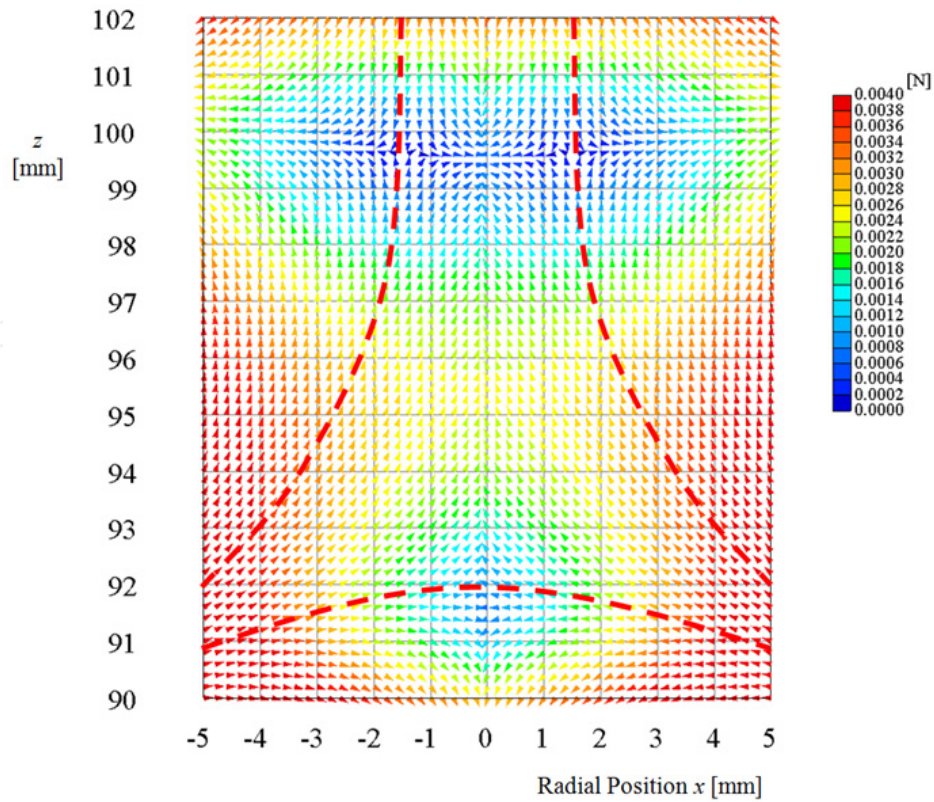
(d) The levitating area when the tilt angle is 1.2°.
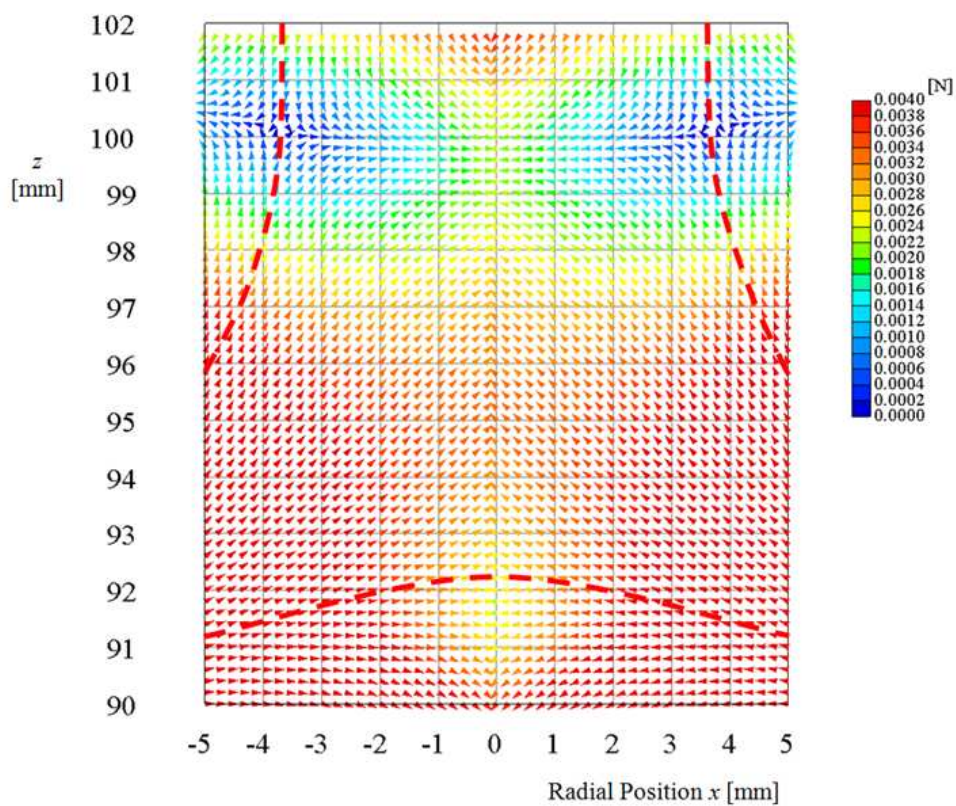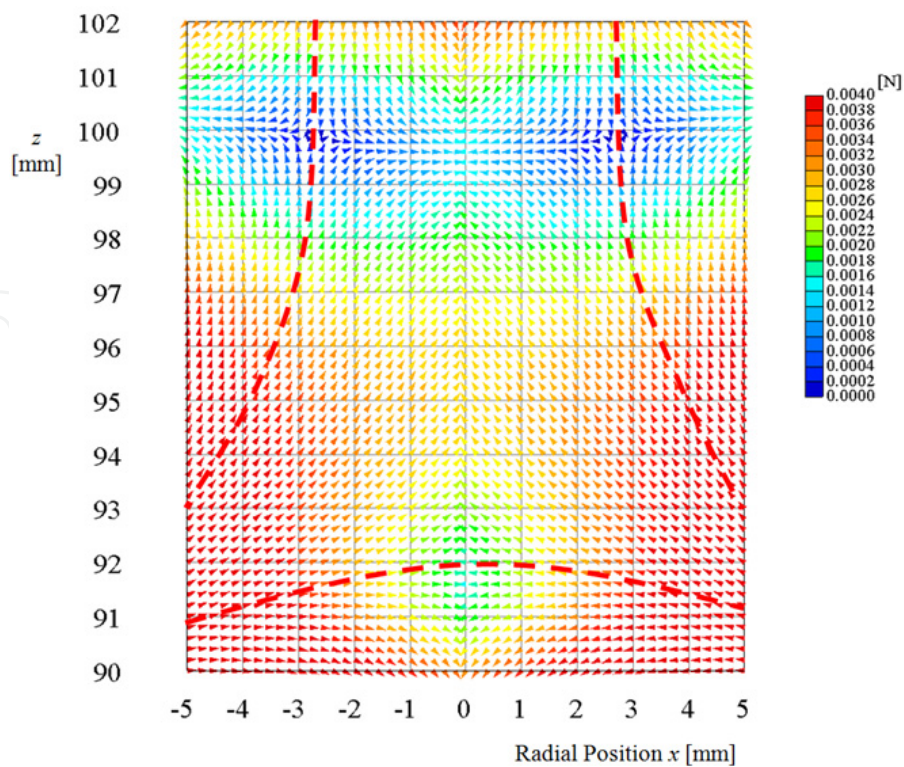
Figure 10. Relationship between the levitating area and the tilt angle of the rotor magnet.

4. Study of the dynamic behaviour of a magnetic top by three-dimensional analysis

We can obtain approximate guidelines for the size and shape of the levitating area by quasi-three-dimensional analysis. Although the static analysis gives the 'levitating area', a magnetic top in this area may not always continue to levitate, considering the dynamic motion of the top. Furthermore, the static analysis mentioned in the previous section showed that the magnitude of the restoring force acting on the rotor magnet was small. Because the quasi-three-dimensional static analysis provides an approximate design of the magnetic top, the three-dimensional dynamic analysis should be performed to confirm whether the rotating magnetic top can maintain levitation.

In this section, how the parameters such as rotating speed, mass of the top and initial position with regard to the restoring centre affect the behaviour of the levitating magnetic top is discussed.

4.1. Effects of rotating speed

To realise a successful rotation of a magnetic top, the rotation speed is one of the most important parameters. Simulated results show that the magnetic top (Table 1) can maintain levitating while it rotates in the range of 18–50 rps, *i.e.* 1,080–3,000 rpm, when the initial position is 1 mm apart in both radial and vertical directions from the restoring centre.

Figures 11(a) and (b) show the trajectories of the centre of the magnetic top rotating at 1020 rpm and 3240 rpm, respectively. This characteristic is closely related to the tilt angle of the rotor magnet, that is, the rotor magnet with the shaft rotating at very low speed cannot maintain an adequate tilt angle because of the lack of mechanical inertia and the rotor magnet with the shaft rotating at a very high speed cannot maintain its tilt angle stable because of the increasing centrifugal force.
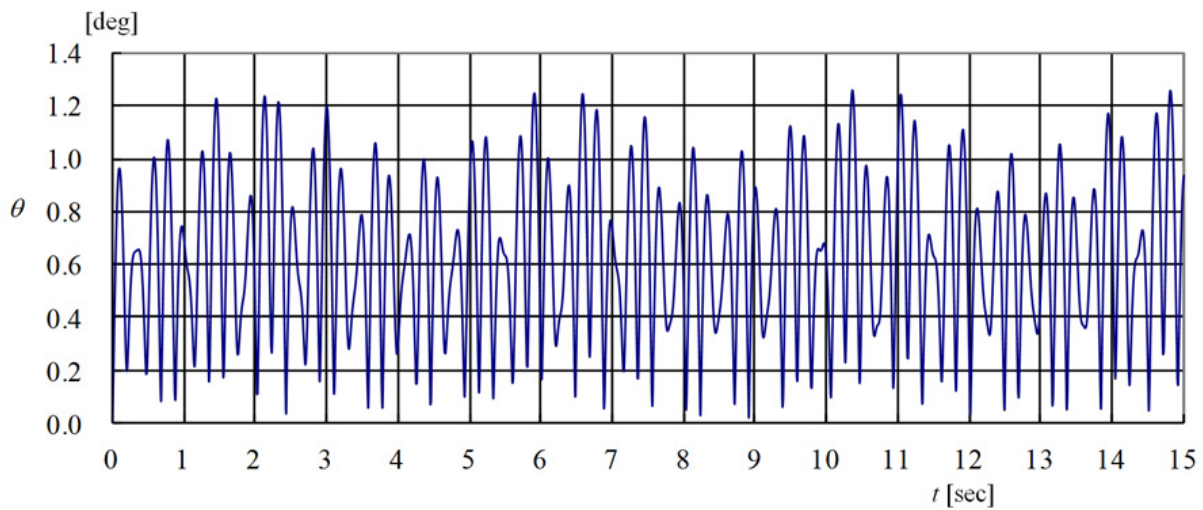
Figure 12 shows the typical time dependency of the tilt angle of the rotor magnet. The tilt angle in this figure indicates the absolute values, *i.e.* the rotor magnet is tilting in a radial direction around z-axis. As shown in this figure, the tilt angle θ varies within 1.2° while the rotor magnet levitates with precession, as in this case. The maximum value of the tilt angle increases with increase in the rotation speed of the rotor magnet, as shown in Figure 13. In this analytical model, the gravity centre of the magnetic top is located at a little upper point along its shaft from the centre of the rotor magnet; therefore, the tilt angle becomes larger with an increase in the rotating speed. Then, the rotor magnet will be thrown in the radial direction, along the magnetic force vectors shown in Figure 10(a). If we design a magnetic top with the gravity centre located at the centre of the rotor magnet, the rotor magnet will rotate without tilting because of its mechanical inertia; however, such a rotor magnet cannot realise levitation, according to previous discussions.

Figure 14 shows the simulated trajectories of a levitating magnetic top rotating at 1,080 rpm for 60 s after starting from point (1, 0, 98.5), which is 1 mm apart from the restoring centre in
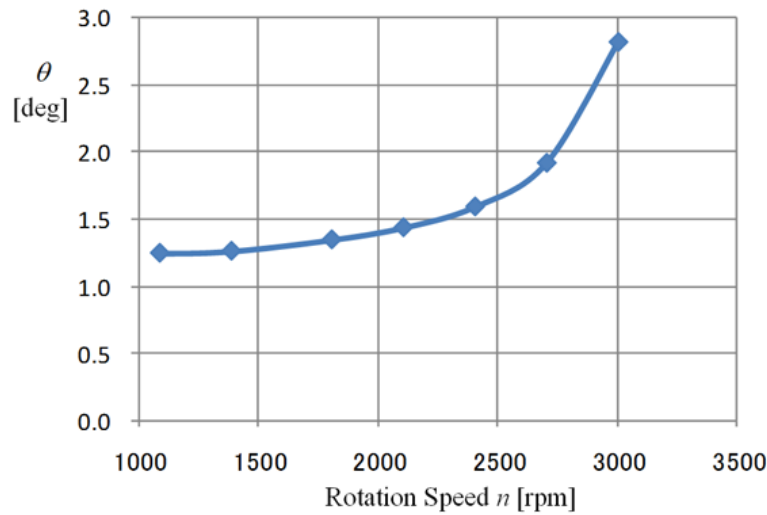
both x and z directions. Figures 14(a) and (b) show the trajectories of the head of the 25 mm long shaft of the magnetic top and Figures 14(c) and (d) show the trajectories of the centre of the rotor magnet. Figures 14(a) and (b) show that the shaft head rotates with both smaller radius nutation and larger radius precession. On the other hand, Figures 14(c) and (d) show that the centre of the rotor magnet rotates with precession when the tilt angle varies periodically. Comparing these two figures, it is observed that a magnetic top, rotating at a low speed such as 1,080 rpm, is rotating in a complex motion with nutation mode in addition to precession mode [6].

(a) Rotating speed: 1020 rpm   (b) Rotating speed: 3240 rpm
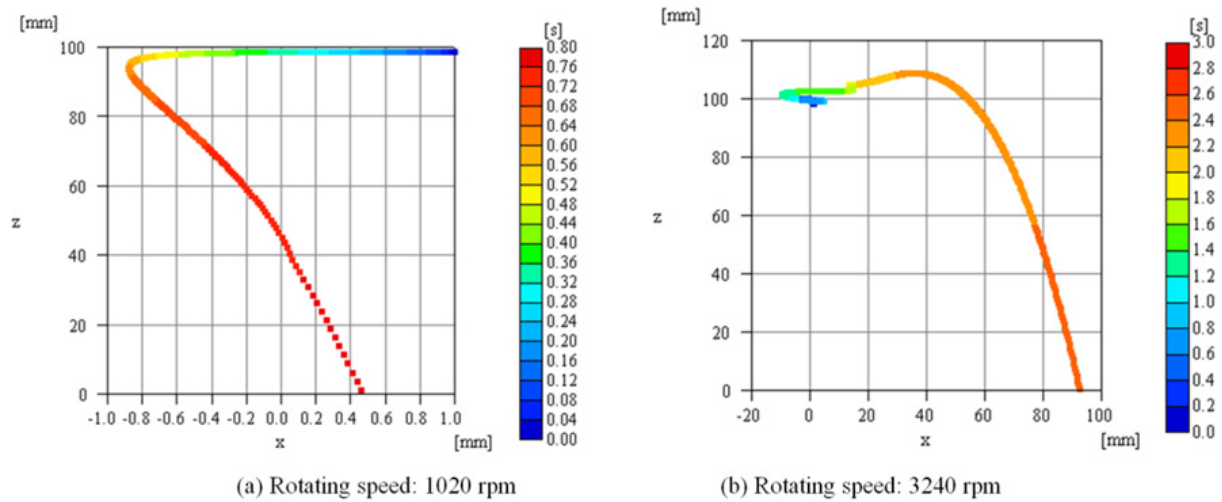
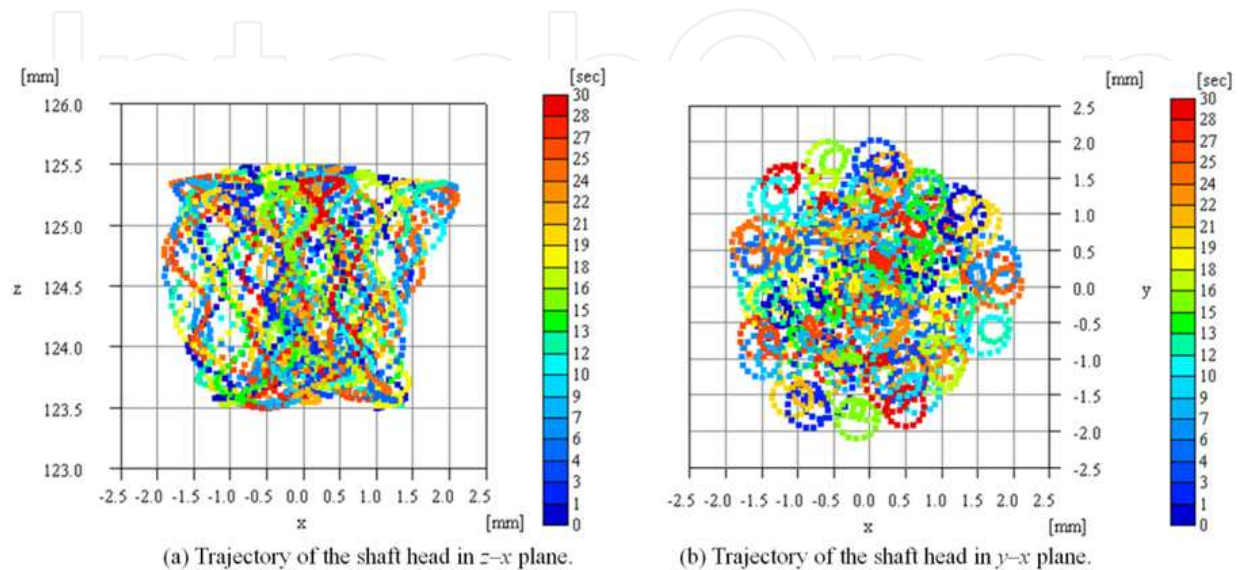**Figure 11.** Trajectories of the magnetic top for 5 s.

Figure 12. Time dependency of the tilt angle of the rotor magnet.

Figure 13. The maximum tilt angle θ vs. rotating speed.

Figure 15 shows the simulated trajectories of a levitating magnetic top rotating at 3,000 rpm for 60 s after starting at point (1, 0, 98.5). Figures 15(a) and (b) show the trajectories of the head of the 25 mm long shaft of the magnetic top and Figures 15(c) and (d) show the trajectories of the centre of the rotor magnet. From these figures, we can observe that both the trajectories of the shaft head and the centre of the rotor magnet are almost the same in shape. However, the shaft head rotates in a little wider range compared to the moving area of the centre of the rotor magnet. This means that a magnetic top rotating at a relatively higher speed, e.g. 3,000 rpm, maintains its levitation with precession mode. In this case, nutation mode is hardly observed.

Although it is difficult to repeat the experiments in the same conditions, these simulated results showed good accordance with the experiments [6].
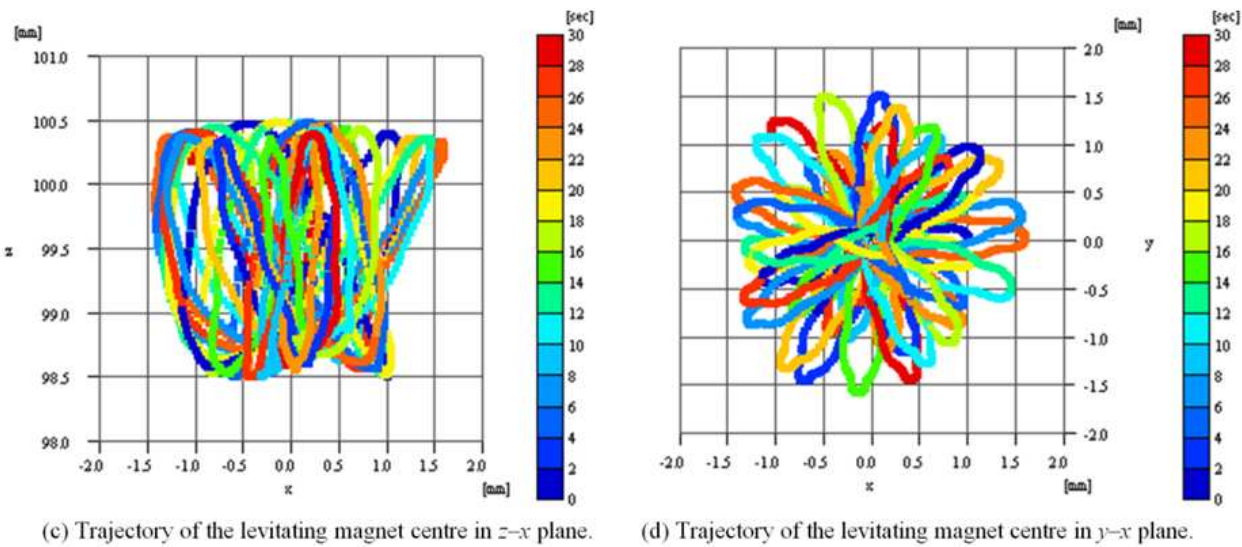

(a) Trajectory of the shaft head in z–x plane.

(b) Trajectory of the shaft head in y–x plane.

(c) Trajectory of the levitating magnet centre in z–x plane.

(d) Trajectory of the levitating magnet centre in y–x plane.

Figure 14. Simulated trajectories of the levitating magnetic top rotating at 1,080 rpm.

(a) Trajectory of the shat head in z–x plane.

(b) Trajectory of the shaft head in y–x plane.

(c) Trajectory of the magnetic centre in z–x plane

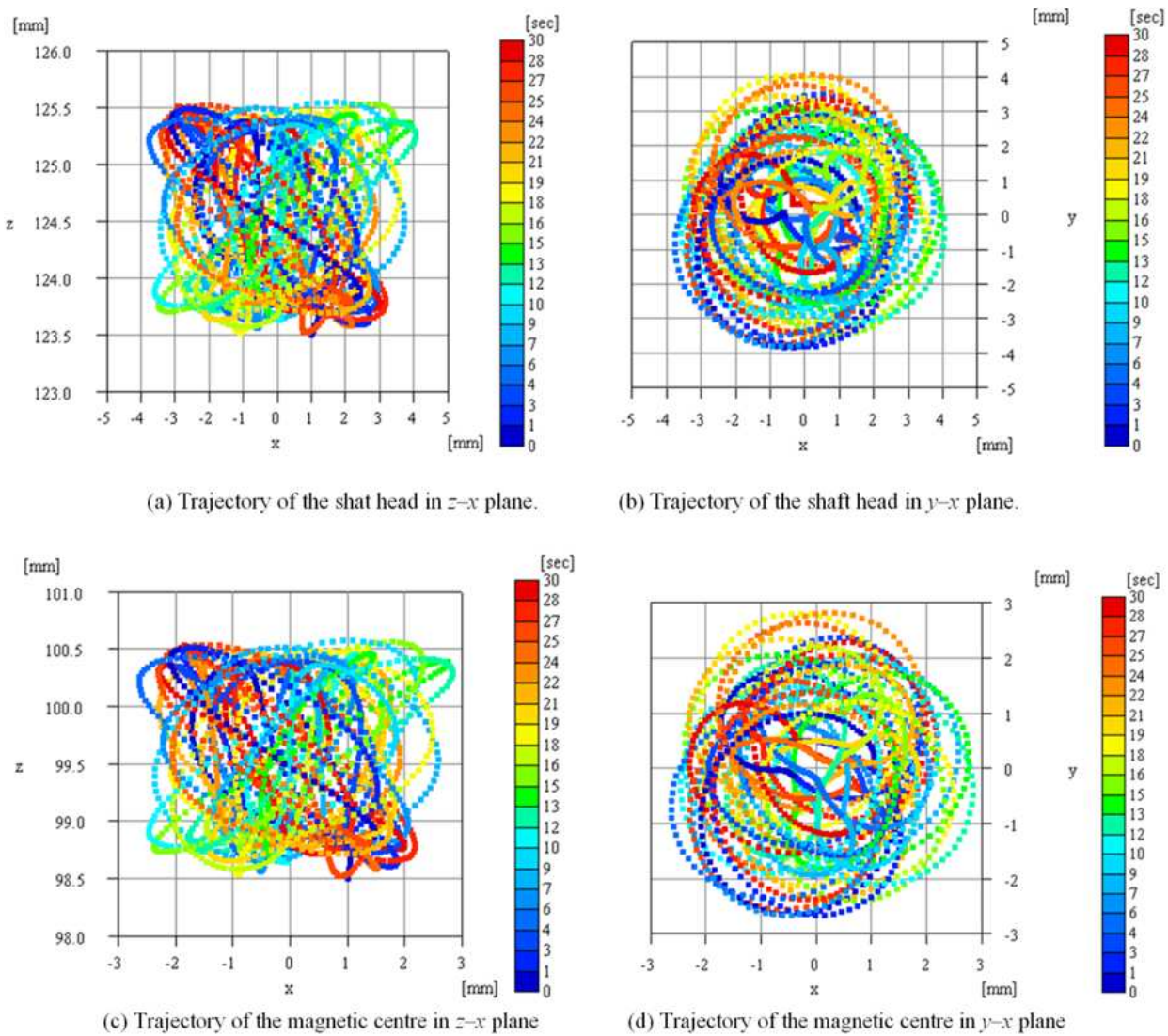(d) Trajectory of the magnetic centre in y–x plane

**Figure 15.** Simulated trajectories of the levitating magnetic top rotating at 3,000 rpm.

4.2. Effects of the mass of a magnetic top and thickness of the stator magnet

In this section, the effects of the mass of a levitating top and the thickness of the stator magnet to the height of the restoring centre are discussed.

Figure 16 shows the relationship between the height of the restoring centre z_r [mm] and the mass of a levitating top m [g] when the thickness of the stator magnet is $h = 60, 40$ and 20 mm. Calculated results show that the height of the restoring centre z_r decreases with an increase in the mass of the top and a decrease in the thickness of the stator magnet.

Calculations were made for various values of the mass of the top in the analytical model described in Table 1. However, there is no restoring centre or levitation area for a heavier or a lighter top than those shown in Figure 16. According to these results, a thin stator magnet may realise successful levitation for wider mass variations.
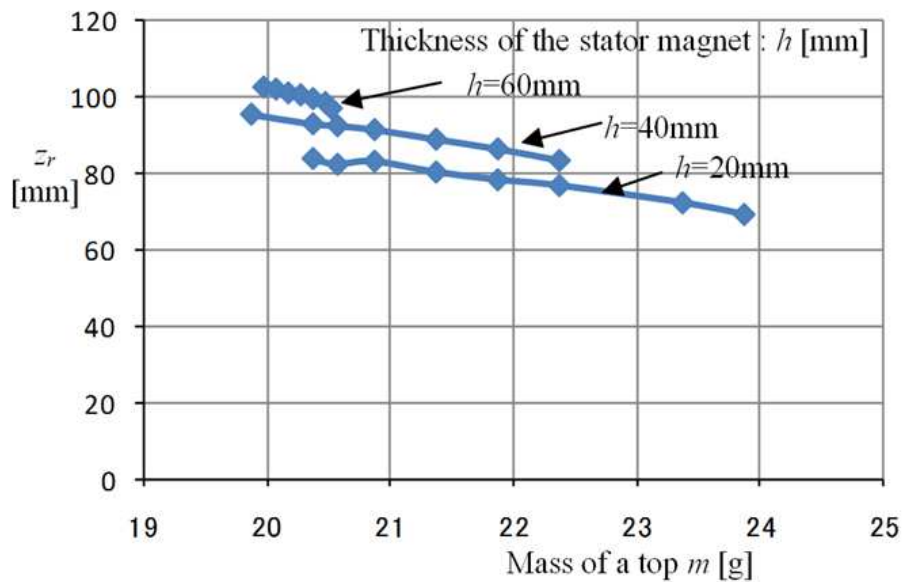
Figure 16. Height of the restoring centre vs. mass of levitating top.

4.3. Effects of the initial position

Some experiments demonstrated that the initial position related to the restoring centre is one of the most important parameters. To realise successful rotation of a magnetic top, the initial position should be at least inside the levitating area defined in the previous section. The magnetic top shows various behaviours according to its initial point with regard to the restoring centre.

Figure 17 shows the simulated trajectory of the centre of the rotor magnet for 60 s starting from (1, 0, 98.5), which is 1 mm apart in both x and z directions from the restoring centre. The mass of the top is 20.37 g and rotation speed is 23 rps, *i.e.* 1380 rpm. These results show that the rotating top is levitated in the area of ±1.6 mm in both x and y directions and of ±1 mm in z direction, from the restoring centre. The maximum tilt angle is 1.26° with the z-axis.

To investigate the effects of the initial point with regard to the restoring centre (0, 0, 99.5), simulations were performed for the case of the typical initial point of (1, 0, 99.5), *i.e.* 1 mm apart in x direction from the restoring centre, and (0, 0, 98.5), *i.e.* 1 mm apart in z direction from the restoring centre. Figures 18(a) and (b) show the simulated trajectories of the centre of the rotor magnet, rotating at 1,380 rpm for 60 s starting from (1, 0, 99.5) and (0, 0, 98.5), respectively.
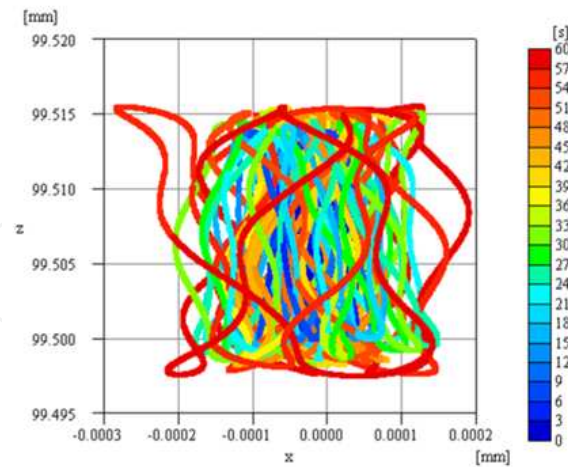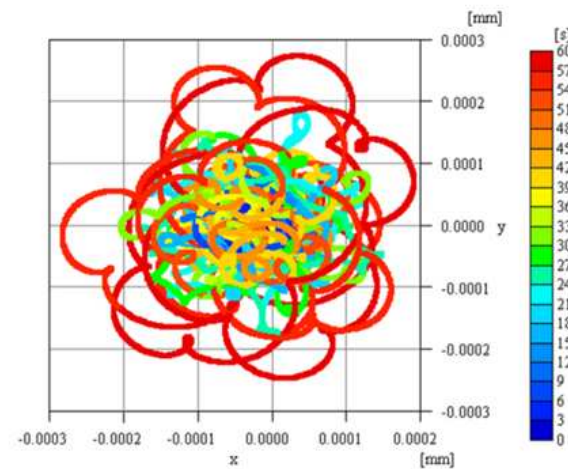
The magnetic top, starting from the point 1 mm apart in x direction from the restoring centre, levitates in the range of ±1.07 mm in both x and y directions and from +0.12 mm/ to 0.06 mm in z direction around the restoring centre, as shown in Figure 18(a). The maximum tilt angle is 1.018°.

(a) Trajectory in z–x plane　　　　　　(b) Trajectory in y–x plane
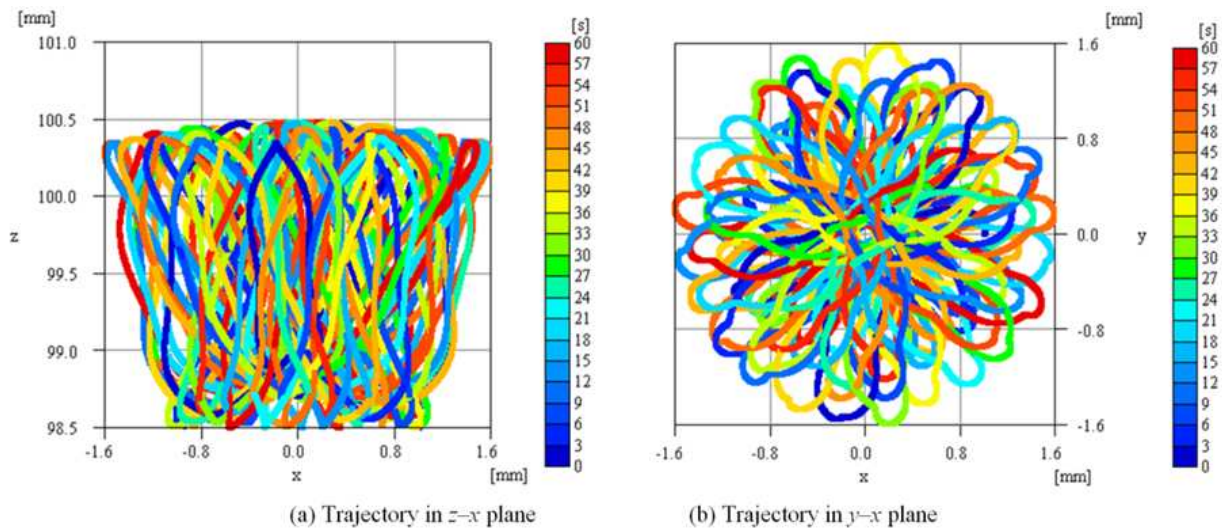
Figure 17. Simulated trajectories of a magnetic top in 60 s starting from (1, 0, 98.5), 1380 rpm.

(a) Trajectory of the rotor magnet starting from (1, 0, 99.5)　　　(b) Trajectory of the rotor magnet starting from (0, 0, 98.5)
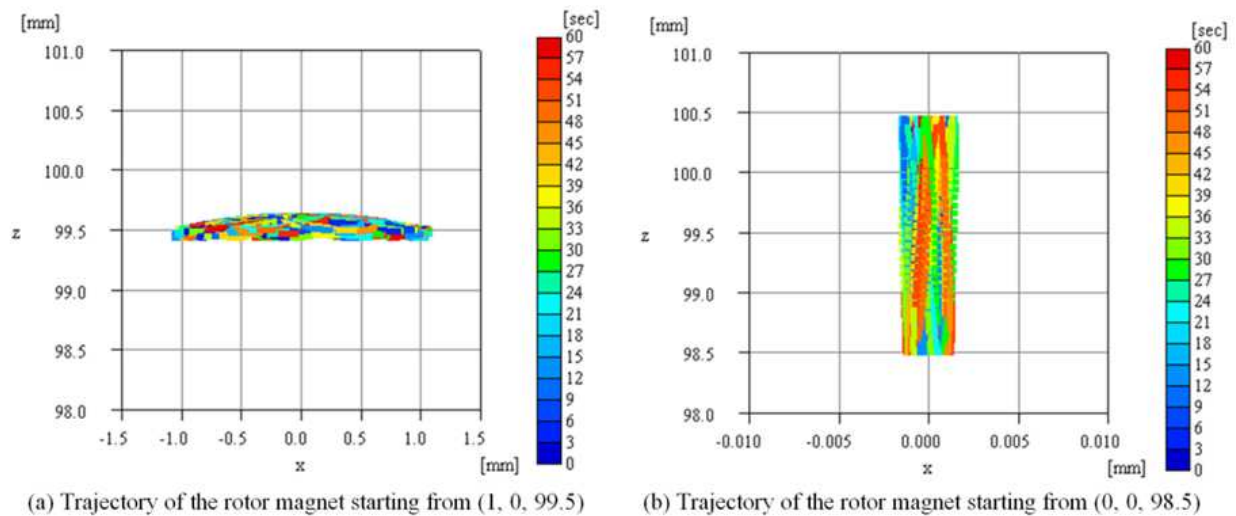
Figure 18. Trajectories of the centre of the rotor magnet in z–x plane.

(a) Trajectory in z–x plane

(b) Trajectory in y–x plane

Figure 19. Trajectories of the rotor magnet centre for 60 s starting from the restoring centre (0, 0, 99.5)

In contrast, the magnetic top, starting at the point 1 mm apart in z direction from the restoring centre, levitates in the range of ±0.002 mm in both x and y directions and ±1 mm in z direction around the restoring centre, as shown in Figure 18(b). The maximum tilt angle is 0.001165°.

Figure 19 shows the simulated trajectory of the centre of the rotor magnet, rotating at 1,380 rpm for 60 s starting from the restoring centre (0, 0, 99.5). In this case, a magnetic top levitates in the area of ±0.0003 mm in x–y plane and +0.016 mm/−0.003 mm in z direction. These results show that a rotating magnetic top can maintain levitation within several micrometres displacements in both radial and vertical directions.

Thus, the magnetic top has the ability to function as an entirely passive magnetic bearing [7].

4.4. Effects of the air drag force

In the previous analysis, the aerodynamic effects were neglected to simplify the discussion. If a magnetic top is rotating in air, rotating speed of the top will decay because of the pneumatic resistance acting on the surfaces of the top. In actual, the experiments showed that the rotating speed of the magnetic top decreases as time passes and the attitude of the top changes to a larger precession that leads it to fall down in a few minutes. Because there are no conducting materials in the magnetic top, there is no electrodynamic drag force caused by eddy currents. Hence, the aerodynamic drag force can be considered as the main reason for the decreasing rotation speed. In this section, some simulations are performed based on the equations of motion considering the aerodynamic drag force.

The aerodynamic effects to the behaviour of a rotating magnetic top is estimated as the pneumatic resistance acting on the outer side surface of the magnetic top. Here, the aerodynamic drag effects caused by the pole surfaces of the magnetic top are neglected. The following expressions are added to estimate the aerodynamic effects to the rotating speed of the magnetic top:

$$\omega_{n+1} = \omega_n - \frac{F_d}{I_{Top}} dt \tag{15}$$

$$F_d = \frac{1}{2} \rho C_d A_r v_r^2 r_{ro} \tag{16}$$

where ρ = 1.225 kg/m³ is the density of air, C_D is the coefficient of pneumatic resistance, A_r = $2\pi r_{ro} h$ is the area of the outer side surface of the top and $v_r = r_{ro}\omega$ is the velocity of the outer side surface of the rotating top [8].

(a) $C_D = 0.5$ (b) $C_D = 5.0$
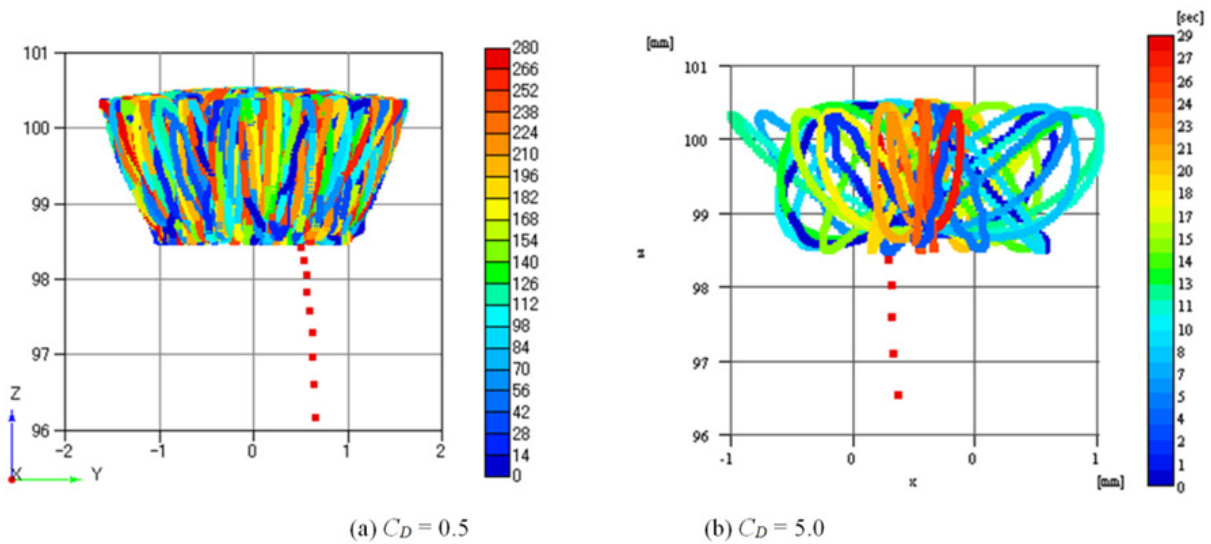
Figure 20. Simulated trajectory of the levitating magnet centre, initial rotating speed is 1380 rpm.

(a) Rotating speed of a magnetic top vs. time.　　(b) Tilt angle of a magnetic top vs. time.
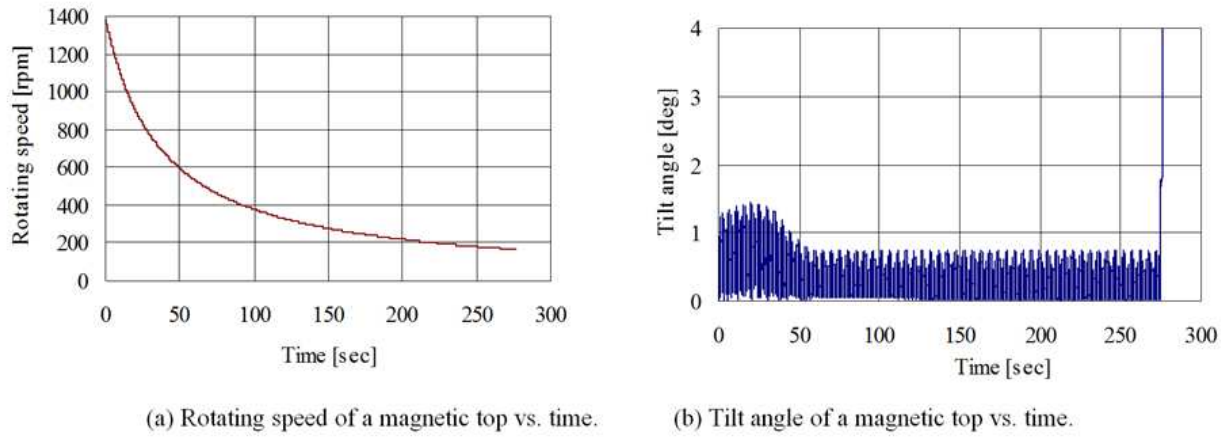
Figure 21. Time dependence of rotating speed and tilt angle of a levitating magnetic top.

(a) Trajectory of the shaft head in the final 15 s.　　(b) Trajectory of the centre of the rotor magnet.
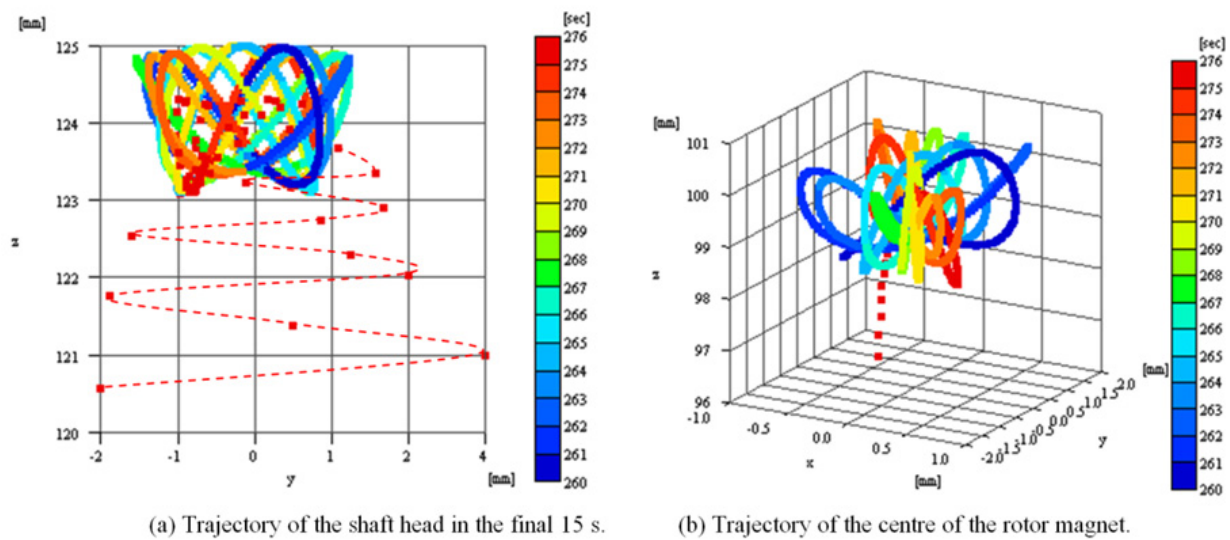
Figure 22. Trajectories of a levitating magnetic top started at 1380 rpm and fall down at 275 s after start.

Figure 20 shows the simulated trajectory of the centre of the levitating magnet starting from 1 mm apart in both x and z directions from the restoring centre. Initial rotation speed is set to be 1,380 rpm. The coefficient of pneumatic resistance C_D is set to be 0.5 for Figure 20(a) and 5.0 for Figure 20(b). Figure 20 shows that the magnetic top can levitate for 275 s or 28.4 s, if the coefficient of pneumatic resistance C_D is 0.5 or 5.0, respectively. Experiments showed that the magnetic top can be levitated for 3–4 min. Hence, in this study, the coefficient of pneumatic resitance C_D is assumed to be 0.5.

Figure 21 shows the time dependence of the rotation speed and the tilt angle of the levitating magnetic top. Figure 21(a) shows that the magnetic top started at 1,380 rpm and maintained levitation till 166 rpm at 275 s.

Figure 21(b) shows the time dependence of the tilt angle of the rotor magnet with respect to *z*-axis. This figure shows that the tilt angle varies within 1.4° while the top is levitating and indicates that precession is needed to maintain levitation for a magnetic top.

Figure 22 shows the trajectories of the magnetic top at the last 15 s of its levitation. Figures 22(a) and (b) demonstrate the trajectories of the shaft head and the centre of the levitating rotor magnet in its final 15 s levitation. These figures show that the precession quickly becomes larger once the magnetic top exits the levitating area.

5. Conclusions

A magnetic top levitates by itself, without any active control system, so long as it rotates in a certain speed range. The authors propose a simple and intuitive analysing method to predict characteristics of the magnetic top.

The quasi-three-dimensional static analysis, considering shapes and layout of the ring-shaped rotor and stator magnets, is used to explain the principle of levitation and obtain the preliminary design parameters of the rotor and stator magnets. The behaviour of the magnetic top is also investigated by dynamic simulations based on the three-dimensional equations of motion considering the moment of inertia for the rotating magnetic top. The following results are obtained:

1. A magnetic top can levitate when it rotates in precession mode with a slight tilting angle and in a certain rotating speed range.
2. The effects of the parameters, such as outer and inner diameters of the rotor and stator magnets, to the behaviour of the magnetic top can be discussed by the quasi-three-dimensional static analysis.
3. A magnetic top rotating at a low speed levitates in both precession and nutation modes. On the contrary, a magnetic top rotating at a high speed levitates with precession, and nutation mode is not observed.
4. The lowest rotation speed is determined to maintain the attitude of the rotating magnet using its mechanical inertia. The maximum rotation speed is limited by the centrifugal force that increases the tilt angle of the shaft of the magnetic top.
5. A magnetic top starting its rotation at the restoring centre will maintain its position with the accuracy of several micrometres.
6. It is difficult to repeat experiments of a magnetic top in the same conditions. However, the proposed analytical results showed good accordance with the experimental data observed using a digital video camera.

A magnetic top may be used as a rotating demonstration model in which some swaying motion can be permitted such as in toys or other relaxation items. When a magnetic top is used in commercial system, a rotor should be rotated by some non-contact drive mechanism such as electric motor or air turbine, etc. Furthermore, touch down bearing should be equipped to suspend a rotor while rotating speed is out of operating range. Fundamental requirements to design a magnetic bearing based on the principle of a magnetic top will be

rotor weight and rotation speed. A rotor shaft should be designed considering mechanical requirements such as torque.

In the experimantal model, because ferrite magnets are used for the rotor and stator magnets, the restoring forces are very small for commercial applications. However, if rare earth permanent magnets and rigid suspension devices are used, sufficient restoring forces may be expected to be generated for use as a commercial passive magnetic bearing.

Author details

Teruo Azukuzawa
Japan Transport Safety Board, Tokyo, Japan

Shigehiro Yamamoto
Graduate School of Maritime Sciences, Kobe University, Kobe, Japan

Acknowledgement

6. References

[1] The Magnetic Levitation Technical Committee of the IEEJ (1993) Magnetic Suspension Technology - Magnetic Levitation Systems and Magnetic Bearings. Corona Publishing Co. Ltd., in Japanese.

[2] Matsumoto M, Azukizawa T (2004) Characteristics of Magnetic Guidance Force Between Coaxial Ring Shaped Permanent Magnets. IEEJ Technical Meetings on Linear Drives, LD-04-93, in Japanese.

[3] Miguel A.S. et al. (2005) Numerical integration for the dynamics of the heavy magnetic top. Physics Letters A 335 235–244.

[4] Ebihara D , Suzuki T (1988) The Repulsive Characteristics of the PM Type Magnetic Levitation Devices. Trans. IEEJ, Vol.108-D, No.5, 455-461, in Japanese.

[5] Azukizawa T, Matsuo N (2007) Feasibility Study of a Magnetic Top As a Magnetic Bearing. Proc. of the 6th International Symposium on Linear Drives for Industrial Applications, LDIA 2007(CD), 138.

[6] Azukizawa T, Yamamoto S, Matsuo N (2008) Feasibility Study of a Passive Magnetic Bearing Using the Ring Shaped Permanent Magnets. IEEE Trans. on Mag., Vol.44, No.11, 4277-4280.

[7] Azukizawa T, Yamamoto S, Makino H (2008) Effects of the System Parameters to the Behavior of a Magnetic Top. MAGLEV08, No. 63.

[8] Azukizawa T, Yamamoto S, Makino H (2009) Analysis of Dynamic Behavior of a Magnetic Top Considering Aerodynamic Drag Force. LDIA2009